PART 1

SOLAR MODELLING

https://doi.org/10.1017/S0252921100067798 Published online by Cambridge University Press

THE STANDARD SOLAR MODEL

J.N.BAHCALL
Institute for Advanced Study
NJ 08540, Princeton
USA
M. CRIBIER
CEN SACLAY DPhPE/SEPh
F-91191 GIF-sur Yvette CEDEX
France

ABSTRACT. The main features of standard solar models, the logic of the calculations, and some of the important results concerning solar neutrinos experiments are given. The input parameters that cause the greatest uncertainties in the calculated neutrino fluxes are the nuclear rection rates, the chemical abundances, the radiative opacity, and the equation of state. This article is based, with permission of the publisher, on Chapters 1 and 4 of *Neutrino Astrophysics* by J. N. Bahcall, Cambridge University Press (1989).

1. Introduction

The Sun is an astronomical laboratory. Because of its proximity to the Earth, we are able to obtain information about the Sun that is not accessible for other stars. We can determine precise values for the solar mass, radius, geometric shape, photon spectrum, total luminosity, surface chemical composition, and age. In addition, astronomers have measured accurate frequencies for thousands of acoustic oscillation modes that are observed at the solar surface. These frequencies contain information about the solar interior. We are beginning to measure the spectrum of neutrinos produced by nuclear reactions in the solar interior. The geological records, the planets, comets, and meteorites, provide information about the past history of the Sun. Taken together, this treasure of experimental information provides a unique opportunity to test theories of stellar structure and evolution.

For two decades, the only operating solar neutrino experiment yielded results in conflict with the most accurate theoretical calculations. This conflict between theory and observation, which has recently been confirmed by a new experiment, is known as the solar neutrino problem. This problem can be stated simply. Both the theoretical and the observational results are expressed in terms of the solar neutrino unit, SNU, which is the product of a characteristic calculated solar neutrino flux (units: cm^{-2} s^{-1}) times a theoretical cross section for neutrino absorption (unit: cm^2). A SNU has, therefore, the units of events per target atom per second and is chosen for convenience equal to $10^{-36}s^{-1}$.

The predicted rate for capturing solar neutrinos in a ^{37}Cl target is

$$\text{Predicted rate} = (7.9 \pm 2.6)\ \text{SNU}, \tag{1a}$$

where the indicated uncertainty represents the total theoretical range including three standard deviation (3σ) uncertainties for measured input parameters. The rate observed

G. Berthomieu and M. Cribier (eds.), Inside the Sun, 21–41.

by Davis and his associates in a chlorine radiochemical detector is

$$\text{Observed rate} = (2.3 \pm 0.75)\ \text{SNU}, \tag{1b}$$

where the error is again a 3σ uncertainty [Davis (1989)].

There is no generally accepted solution to the discrepancy although a number of interesting possibilities have been proposed.

This discrepancy between calculation and observation has recently been confirmed by an independent technique using the Japanese detector of neutrino–electron scattering, Kamiokande II. The recent Kamiokande II result is [Hirata et al. (1989)]

$$\frac{\phi_{\text{observed}}}{\phi_{\text{predicted}}} = 0.39 \pm 0.09(stat.) \pm .06(syst.), \tag{2}$$

where the neutrino flux, ϕ, is from the rare ^{8}B solar neutrinos and the quoted error is the 1σ uncertainty.

The predictions used in Eqs. (1) and (2) are valid for the combined standard model, that is, the standard model of electroweak theory (of Glashow, Weinberg, and Salam) and the standard solar model.

The presentation given here is based upon the results of Bahcall and Ulrich (1988) and Bahcall (1989), as well as the references cited in this article. In a recent detailed study, Sienkiewicz, Bahcall, and Pacynski (1989) constructed a standard solar model using an independently developed numerical code. Adopting the standard model input parameters, the authors obtain 7.6 SNU for the calculated absorption rate in the ^{37}Cl experiment. The difference of 0.3 SNU between this result and the Bahcall-Ulrich value given earlier is due to the combined effect of several small differences in physical description that were to time-consuming to incorporate in the Sienkiewicz et al. code. Turck-Chièze et al. (1988) describe the result of a calculation in which they do not use modern standard input parameters for the ^{8}B nuclear production cross section and for the opacity. They choose to use a nuclear cross section that is different from that reported by the experimentalists in all the recent reviews [see for example Parker and Rolfs (1989) or Parker (1986)] and opacities that were computed more than a decade ago. Their results demonstrate that one can obtain different answers for the predictions of solar models (within the acknowledged uncertainties) by choosing different input parameters.

In section 2, the input parameters of the standard models are presented. The pp chain which is the dominant source of the energy for the sun is described in section 2.1. Neutrino interaction cross, section (2.2), permit the prediction of the rate in specific detectors. Chemical abundances (section 2.3), opacities (2.4), and the equation of states, (2.5), are described to indicate their contributions to the uncertainties of the calculations.

Section 3 describes the general method used in the computation of the solar standard model. The basic equations (3.1) with the main physical hypothesis are used in the calculation procedure (3.2). The main characteristics resulting from this computation are presented in section 4.

Prediced rates for the different solar neutrinos experiments are compared with the experimental results in section 5. The section 6 points out some features of the solar standard model related to helioseismology.

Table 1. Some important solar quantities. The measured parameters are: photon luminosity, mass, radius, oblateness, and age. All other quantities are calculated with the aid of the standard solar model.

Parameter	Value
Photon luminosity ($L_\odot$)	3.86×10^{33} erg s^{-1}
Neutrino luminosity	$0.023 L_\odot$
Mass ($M_\odot$)	1.99×10^{33} g
Radius ($R_\odot$)	6.96×10^{10} cm
Oblateness $[(R_{\text{equatorial}}/R_{\text{polar}}) - 1)]$	$\leq 2 \times 10^{-5}$
Effective (surface) temperature	5.78×10^3 K
Moment of inertia	7.00×10^{53} g cm^2
Age	$\approx 4.55 \times 10^9$ yr
Initial helium abundance by mass	0.27
Initial heavy element abundance by mass	0.020
Depth of convective zone	$0.26 R_\odot (0.015 M_\odot)$
Central density	148 g cm^{-3}
Central temperature	15.6×10^6 K
Central hydrogen abundance by mass	0.34
Neutrino flux from pp reaction	6.0×10^{10} cm^{-2} s^{-1}
Neutrino flux from ^{8}B decay	6×10^6 cm^{-2} s^{-1}
Fraction of energy from pp chain	0.984
Fraction of energy from CNO cycle	0.016

2. The input parameters

The major input parameters or functions that are used in a standard solar model are: nuclear parameters, solar luminosity, solar age, equation of state, elemental abundances, and radiative opacity.

Table 1 lists some of the main physical characteristics of the Sun. Of special importance for the solar neutrino problem are the accurately determined luminosity and mass, the initial heavy element to hydrogen ratio (Z), and an upper limit on the intrinsic solar oblateness [Dicke, Kuhn, and Libbrecht (1985)].

2.1 Nuclear energy generation and neutrino fluxes

The Sun shines by converting protons into α-particles. About 600 million tons of hydrogen are burned every second to supply the solar luminosity. Nuclear physicists have worked for half a century to determine the details of this transformation. The subject has been recently reviewed by Parker and Rolfs (1989). From the uncertain parameters in nuclear cross section, Bahcall and Ulrich (1988) derived uncertainties of 1.7 SNU for the ^{37}Cl experiment and 7 SNU for the ^{71}Ga experiments.

The main nuclear burning reactions in the Sun are shown in Table 2, which represents the energy-generating **pp chain**. This table also indicates the relative frequency with which each reaction occurs in the standard solar model.

The fundamental reaction in the solar energy-generating process is the proton–proton (pp) reaction. In the pp reaction, a proton β-decays in the vicinity of another proton

https://doi.org/10.1017/S0252921100067798 Published online by Cambridge University Press

Table 2. The pp chain in the Sun. The average number of pp neutrinos produced per termination in the Sun is 1.85. For all other neutrino sources, the average number of neutrinos produced per termination is equal to (the termination percentage/100).

Reaction	Number	Termination† (%)	ν energy (MeV)
$p + p \rightarrow {}^2H + e^+ + \nu_e$	1*a*	100	≤ 0.420
or			
$p + e^- + p \rightarrow {}^2H + \nu_e$	1*b* (pep)	0.4	1.442
${}^2H + p \rightarrow {}^3He + \gamma$	2	100	
${}^3He + {}^3He \rightarrow \alpha + 2p$	3	85	
or			
${}^3He + {}^4He \rightarrow {}^7Be + \gamma$	4	15	
${}^7Be + e^- \rightarrow {}^7Li + \nu_e$	5	15	(90%) 0.861 (10%) 0.383
${}^7Li + p \rightarrow 2\alpha$	6	15	
or			
${}^7Be + p \rightarrow {}^8B + \gamma$	7	0.02	
${}^8B \rightarrow {}^8Be^* + e^+ + \nu_e$	8	0.02	< 15
${}^8Be^* \rightarrow 2\ \alpha$	9	0.02	
or			
${}^3He + p \rightarrow {}^4He + e^+ + \nu_e$	10 (hep)	0.00002	≤ 18.77

†The termination percentage is the fraction of terminations of the pp chain, $4p \rightarrow \alpha + 2e^+ + 2\nu_e$, in which each reaction occurs. The results are averaged over the model of the current Sun. Since in essentially all terminations at least one pp neutrino is produced and in a few terminations one pp and one pep neutrino are created, the total of pp and pep terminations exceeds 100%.

forming a bound system, deuterium (^{2}H). This reaction (number 1*a* in Table 2) produces the great majority of solar neutrinos; however, these pp neutrinos have energies below the detection thresholds for the ^{37}Cl and Kamiokande II experiments. Experiments with ^{71}Ga are sensitive primarily to neutrinos from the pp reaction. More rarely, a three-body reaction involving two protons and an electron initiates the reaction chain. While this reaction (number 1*b* in Table 2) occurs with a relative frequency of only one in 250, the resulting neutrino energy is larger by the equivalent of two electron masses, raising it above the threshold in the chlorine experiment. The deuteron produced by either of the initiating reactions is burned quickly by a (p,γ) reaction that forms ^{3}He (reaction 2 in Table 2). Reactions 1*a* and 2 occur in essentially all terminations of the pp chain in the Sun; reaction 1*b* occurs only rarely, in approximately 0.4% of all pp terminations. The richness and complications of the pp cycle begin at the next stage.

Most of the time, 85% in the standard solar model, the proton–proton chain is terminated by two ^{3}He nuclei fusing to form an α-particle plus two protons (reaction 3 of Table 2). No additional neutrinos are formed in this dominant mode.

About 15% of the time, a ^{3}He nucleus will capture an already existing α-particle to form ^{7}Be plus a gamma ray (reaction 4). It is the neutrinos formed after this process that are primarily detected in the ^{37}Cl experiment. Nearly always, the ^{7}Be nucleus will undergo

https://doi.org/10.1017/S0252921100067798 Published online by Cambridge University Press

electron capture, usually absorbing an electron from the continuum of ionized electrons (reaction 5). This branch produces neutrinos with energies of 0.9 MeV (90% of the time), which contribute small (but not negligible) fractions of the predicted standard model capture rate in the ^{37}Cl and ^{71}Ga experiments. There is no experiment in progress that isolates the contribution of the ^{7}Be neutrinos, although some suggestions for practical detectors have been made.

Most of the predicted capture rate in the ^{37}Cl experiment comes from the rare termination in which ^{7}Be captures a proton to form radioactive ^{8}B (reaction 7). The ^{8}B decays to unstable ^{8}Be, ultimately producing two α-particles, a positron, and a neutrino. The neutrinos from ^{8}B decay have a maximum energy of less than 15 MeV. Although the reactions involving ^{8}B occur only once in every 5000 terminations of the pp chain, the total calculated event rates for the ^{37}Cl and Kamiokande II experiments are dominated by this rare mode.

For ^{37}Cl, the ^{8}B contribution is most important because many of the neutrinos from this source are sufficiently energetic to excite a superallowed transition between the ground state of ^{37}Cl and the analogue excited state of ^{37}Ar (which closely resembles the ground state of ^{37}Cl). None of the more abundant neutrinos have enough energy to cause this strong analogue transition.

The last reaction in Table 2, number 10, is extremely rare, occurring about twice in every 10^{7} terminations of the pp chain. Nevertheless, the neutrinos from this reaction may be detectable in some direct counting electronic experiments (with, e.g., deuterium or ^{40}Ar) because they have the highest energies of any of the sources in Table 2.

The neutrinos from reaction 1*b*, which is initiated by three particles, p+e+p, are known as **pep** neutrinos. The neutrinos from the ^{3}He+p reaction are known as **hep** neutrinos.

The neutrino spectrum predicted by the standard model is shown in Figure 1, where contributions from both line and continuum sources are included. For Kamiokande II, only the ^{8}B and hep neutrinos (reaction 10) have enough energy to produce recoil electrons above the dominant backgrounds.

2.2 Neutrino interaction cross sections

The measured event rate in a solar neutrino experiment is the product of the neutrino flux times the interaction cross sections. The ingredients used in the calculation of neutrino absorption cross sections are discussed in detail in Bahcall (1978), Bahcall (1989). The results of this computation, including contribution from excited states and forbidden effects, as included in Bahcall and Ulrich (1988), is shown in Figure 2, for a ^{37}Cl target and ^{71}Ga target.

Uncertainties on the absorption cross section come from transitions to excited states and from forbidden corrections. The ^{37}Cl experiment benefits from the calibration of the transitions to excited states of ^{37}Ar using data from the decay of ^{37}Ca; the total uncertainties from absorption cross sections is 0.6 SNU. In the ^{71}Ga experiments, the uncertainties are dominated by transitions to excited states for all but pp (dominated by forbidden corrections) , ^{7}Be and ^{13}N sources (not enough phase space above threshold for excited states); the estimated uncertainty is asymmetric +16 SNU -11 SNU.

2.3 Chemical abundances

The chemical abundances of the elements affect the computed radiative opacity and hence the temperature–density profile of the solar interior. The joint efforts of many different

https://doi.org/10.1017/S0252921100067798 Published online by Cambridge University Press

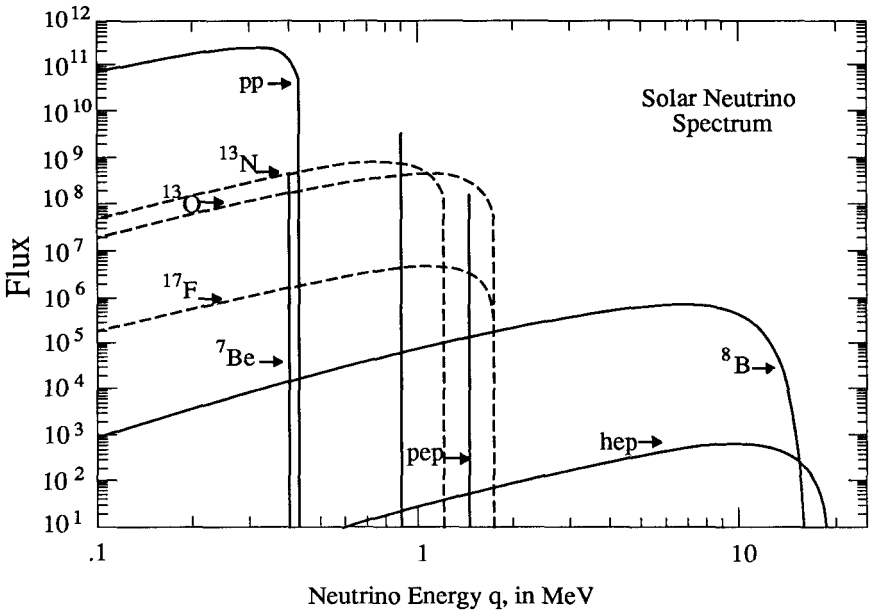

Figure 1. Solar neutrino spectrum. This figure shows the energy spectrum of neutrinos predicted by the standard solar model. The neutrino fluxes from continuum sources (like pp and ^{8}B) are given in the units of number per cm^2 per second per MeV at one astronomical unit. The line fluxes (pep and ^{7}Be) are given in number per cm^2 per second. The spectra from the pp chain are drawn with solid lines; the CNO spectra are drawn with dotted lines. [Reproduced with permission of the publisher from *Neutrino Astrophysics* by J. N. Bahcall, Cambridge University Press (1989).]

researchers has been ably summarized in two reviews one by Grevesse (1984), adopted by Bahcall and Ulrich (1988) and the other by Aller (1986).

The present composition of the solar surface is presumed, in standard solar models, to reflect the initial abundances of all of the elements that are at least as heavy as carbon. The fractional abundance by mass of elements heavier than helium is called the heavy element abundance and is traditionally denoted by Z. The corresponding abundances by mass of hydrogen and helium are denoted by X and Y.

The initial ratio by mass of elements heavier than helium relative to hydrogen, Z/X, is one of the crucial input parameters in the determination of a solar model. The fractional abundances of each of the elements are also important in determining the stellar opacity, which is closely linked to the predicted neutrino fluxes.

Table 3 lists the individual fractional abundances of the heavy elements that are recommended by Grevesse (1984) and Aller (1986). The two studies are in excellent agreement. The Grevesse (1984) value is $(Z/X)_{\rm Grevesse} = 0.02765$ and for the Aller (1986) mixture $(Z/X)_{\rm Aller} = 0.02739$. The difference between the value of Z/X used in old studies [Bahcall (1982)] and the current value of Grevesse (1984) and Aller (1986) is about 19%.

https://doi.org/10.1017/S0252921100067798 Published online by Cambridge University Press

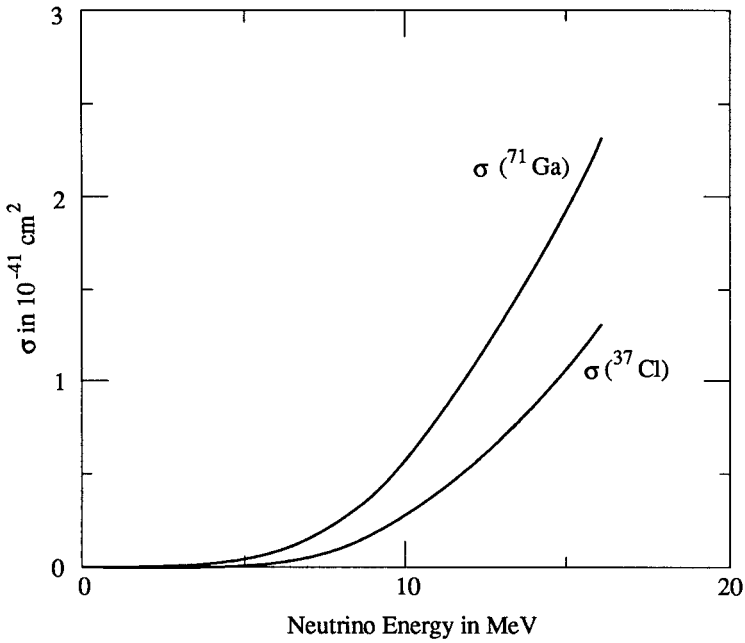

Figure 2. Neutrino absorption cross section. [Reproduced with permission of the publisher from *Neutrino Astrophysics* by J. N. Bahcall, Cambridge University Press (1989).]

Uncertainties due to chemical composition are 1.8 SNU and 10 SNU for ^{37}Cl and ^{71}Ga experiments respectively.

In order to employ these surface abundances in stellar interior calculations, two important but quantitatively plausible assumptions are made. First, the Sun is assumed to be chemically homogeneous when it arrives on the main sequence. Pre-main sequence models of solar type stars are convectively mixed [see Hayashi (1961, 1966)]. Second, the composition of the present solar surface is assumed to reflect the initial abundances of all elements at least as heavy as carbon. Nuclear burning, for material presently confined to the outer parts of the Sun, is negligible because the temperatures within the present convective zone are relatively low.

2.4 The radiative opacity

The transport of energy in the central regions of the Sun is primarily through photon radiation, although electron conduction contributes somewhat in the innermost regions and convection dominates near the surface. The calculated radiative opacity depends upon the chemical composition and upon the modeling of complex atomic processes. The calculations require, for the solar interior, the use of large computer codes in order to include all of the known statistical mechanics and atomic physics [see Huebner (1986)]. The primary source for accurate astrophysical opacities has been, for many years, the Los Alamos National Laboratory codes, presumably developed for related thermonuclear

Table 3. Fractional abundances of heavy elements.

Element	Number fraction [Grevesse (1984)]	Number fraction [Aller (1986)]
C	0.29661	0.27983
N	0.05918	0.05846
O	0.49226	0.49761
Ne	0.06056	0.06869
Na	0.00129	0.00125
Mg	0.02302	0.02552
Al	0.00179	0.00198
Si	0.02149	0.02672
P	0.00017	0.00018
S	0.00982	0.01040
Cl	0.00019	0.00019
Ar	0.00230	0.00227
Ca	0.00139	0.00134
Ti	0.00006	0.00007
Cr	0.00028	0.00035
Mn	0.00017	0.00016
Fe	0.02833	0.02382
Ni	0.00108	0.00114
Total	1.000	1.000

applications [Cox (1989)]; another approach of this problem has been developped at the Lawrence Livermore Laboratory, as explained by Iglesias (1989).

Because the opacity determines in large part the temperature profile, the adopted opacity constitutes an important source of uncertainty for solar neutrino calculations : 0.5 SNU for ^{37}Cl and 3 SNU for gallium experiments. The typical uncertainty is less than 10% .

2.5 The equation of state

The equation of state, the relation between pressure and density, must include accurately the effects of radiation pressure and electron degeneracy [see, e.g., Rakavy and Shaviv (1967) or Schwarzschild (1958)], and screening interactions [according to the Debye–Hückel theory, see footnote 15 of Bahcall and Shaviv (1968)]. All of these effects can be included without unusual complications in a stellar interior code; the remaining recognized uncertainties do not significantly affect the calculated solar structure or the neutrino fluxes [see Bahcall *et al.* (1982) and Ulrich (1982)]. However, numerical experiments show that the computed neutrino fluxes are sensitive to hypothetical localized changes in the equation of state when the perturbations are introduced near 8×10^6K [Bahcall, Bahcall, and Ulrich (1969)].

3. General method

3.1 The ingredients

The standard solar model is calculated using the best physics and input parameters that are available at the time the model is constructed. Thus the set of numbers that correspond to the standard solar model vary with time, hopefully (nearly) always getting closer to the "true" standard model. In the quarter of a century that standard solar models have been used to compute neutrino fluxes, there have been many hundreds of improvements in the input parameters and in the description of the physics. A few seemingly esoteric upgrades of the codes made noticeable differences in the predictions of neutrino fluxes, but a number of the most difficult and careful investigations of new physics or input parameters resulted in little change in the calculated fluxes.

Some of the principal approximations used in constructing standard models deserve special attention since they have been investigated particularly thoroughly or often for possible sources of departure from the standard scenario.

(1) **Hydrostatic equilibrium.** The Sun is assumed to be in hydrostatic equilibrium; the radiative and particle pressures of the model exactly balance gravity.

$$\frac{\mathrm{d}P(r)}{\mathrm{d}r} = -\frac{GM(r)\rho(r)}{r^2}. \tag{3}$$

Observationally, this is known to be an excellent approximation since a gross departure from hydrostatic equilibrium would cause the Sun to collapse in a free-fall time, which is less than an hour. The pressure is the sum of the radiative and the (dominant) thermal pressure:

$$P(r) = \frac{a}{3}T^4 + \frac{1}{\mu}\frac{k\rho T}{m_{\mathrm{H}}}\Big(1 + D\Big). \tag{4}$$

$a = 4\sigma/c$ where σ is the Stefan-Boltzmann constant, k is the Boltzmann's constant and D represents easily calculated corrections for the degeneracy of electrons and for Debye–Hückel modifications to the equation of state. Pulsation, rotation, and pressure due to magnetic fields are all estimated to be unimportant for purposes of calculating solar neutrino fluxes.

(2) **Energy transport by photons or convective motions.** The equation governing energy transport is:

$$L_r = -4\pi r^2(ac/3)\frac{1}{\kappa\rho}\frac{\mathrm{d}T^4}{\mathrm{d}r}. \tag{5}$$

Here L_r is the energy per unit time that passes through a sphere of radius r and T is the temperature. The total opacity κ is the combination of a radiative and a conductive opacity: $\kappa^{-1} \equiv \kappa_{\mathrm{rad}}^{-1} + \kappa_{\mathrm{cond.}}^{-1}$. For solar interior conditions, the radiative opacity dominates the total opacity. For regions that are unstable against convective motions, the temperature gradient is taken to be the adiabatic gradient except near the surface (important for the helioseismological calculations) where mixing length theory is used. Additional transport due to acoustic or gravity waves is negligible in the standard solar model.

(3) **Energy generation by nuclear reactions.** The primary energy source for the radiated photons and neutrinos is nuclear fusion, although small effects of

https://doi.org/10.1017/S0252921100067798 Published online by Cambridge University Press

contraction or expansion are included in the standard solar model. The standard codes include departures from nuclear equilibrium that are caused by the fusion processes themselves, for example, in the abundance of ^{3}He. The rate at which the luminosity is produced in spherical shells is the sum of nuclear ($\epsilon_{\text{nuclear}}$) and mechanical energy generation:

$$\frac{\mathrm{d}L_r}{\mathrm{d}r} = \rho(4\pi r^2)\left(\epsilon_{\text{nuclear}} - T\frac{\mathrm{d}S}{\mathrm{d}t}\right), \tag{6}$$

where S is the stellar entropy.

(4) **Abundance changes caused solely by nuclear reactions.** The primordial solar interior is chemically homogeneous in the standard model. Changes in the local abundances of individual isotopes occur only by nuclear reactions in those regions of the model that are convectively stable. Thermal and gravitational diffusion are not included at present, because they are estimated to be small over the lifetime of the Sun [see Cox, Guzik, and Kidman (1989)].

3.2 Calculational procedure

A standard solar model is the end product of a sequence of models. One begins with a main sequence star that has a homogeneous composition. Hydrogen burns in the deep interior of the model, supplying both the radiated luminosity and the local heat (thermal pressure) which supports the star against gravitational contraction. Successive models are calculated by allowing for composition changes caused by nuclear reactions, as well as the mild evolution of other parameters; the integration of the nuclear abundance equations involves some numerical complications that can be handled best by specialized techniques. The nuclear interaction rates are interpolated between the previous and new models and multiplied by a time step (usually of order 5×10^8 or 10^9 yr.), in order to determine the new chemical composition as a function of mass fraction included. The model at the advanced time is computed using the new composition. The models in an evolutionary sequence have inhomogeneous compositions; in the model for the present epoch, the innermost mass fraction of hydrogen is about one-half the surface (initial) value.

The stellar evolution models are constructed by integrating from the center outward and from the surface inward, requiring that the two solutions match at a convenient point that is typically at about $0.2M_\odot$. Only a relatively crude treatment of the solar atmosphere is required for computing accurate values for solar interior parameters. Even a 10% change in the outer radius of the model does not significantly affect the calculated neutrino fluxes [see Sears (1964) or Bahcall and Shaviv (1968), Eq. (3)]. From time to time, different works in the field have claimed a sensitivity. The difference between the most careful and the crudest treatment of the solar convection zone corresponds to at most a 2% change in the calculated solar neutrino fluxes [see Bahcall and Ulrich (1988), Section X.D]. (As different workers have adapted computer codes from other problems to the calculation of solar neutrino fluxes, they have sometimes reported a sensitivity of the fluxes to the atmospheric model. In all cases, the claimed sensitivity has disappeared as the computer bugs were removed, see Bahcall (1989).)

https://doi.org/10.1017/S0252921100067798 Published online by Cambridge University Press

How does one proceed in practice? One begins by guessing initial values of X, the original homogeneous hydrogen abundance, and S, an entropy-like variable.† Typically, an evolutionary sequence requires of order five to seven solar models of progressively greater ages to match the luminosity and radius to the desired one part in 10^5.

The initial helium abundance of the model Y, is determined in the process of iteration. The other two composition parameters are fixed by the surface ratio of Z/X (heavy elements/hydrogen) that is taken from observations and by the fact that the sum of all the mass fractions is equal to unity, that is, $X + Y + Z = 1.0$.

A satisfactory solar model is a solution of the evolutionary equations that satisfies boundary conditions in both space and time. One seeks a model with a fixed mass $M_\odot$ and with a total luminosity (in photons) equal to $L_\odot$ and an outer radius $R_\odot$ at an elapsed time of 4.6×10^9 yr, the present age of the Sun. The initially assumed values of X (the hydrogen mass fraction) and S (the entropy-like variable) are iterated until an accurate description is obtained of the Sun at the present epoch.

The luminosity boundary condition has an especially strong effect on the calculated neutrino fluxes. The reason is that both the luminosity and the neutrino fluxes are produced by nuclear reactions in the deep solar interior.

4. Some characteristics of the standard model

There are a number of characteristics of the standard model that are of general interest. For example, the fraction of the photon luminosity that originates in the pp chain is 0.984; the corresponding fraction for the CNO cycle is 0.016. The net expansion at the present epoch corresponds to a luminosity fraction of -0.0003. The convection zone terminates at 1.92×10^6 K, corresponding to a radius of about $0.74R_\odot$ and a density of $0.12\,\mathrm{g\,cm^{-3}}$; the convection zone comprises the outer 1.5% of the solar mass.‡ One-half of the photon luminosity (or the flux of pp neutrinos) is produced within the inner $0.09M_\odot$ ($R \leq 0.11R_\odot$); 95% of the photon luminosity is produced within the inner $0.36M_\odot$ ($R \leq 0.21R_\odot$). The neutrino luminosity is 2.3% of the photon luminosity, which corresponds to an average of 0.572 MeV lost in neutrinos per termination of the pp chain. The pp chain is terminated 85.5% of the time by the ^{3}He–^{3}He reaction (number 3 of Table 2) and 14.5% of the time by the ^{3}He–^{4}He reaction (number 4 of Table 2).

Figure 3 illustrates some of the most interesting physical characteristics of the standard solar model. Figure 3*a* shows the fraction of the energy generation that is produced at different positions in the Sun. The energy generation peaks at a radius of $0.09R_\odot$, which corresponds to about $0.06M_\odot$. Figures 3*b* and 3*c* illustrate the distributions of temperature and density; the central values are, respectively, 15.6×10^6 K and $148\,\mathrm{gcm^{-3}}$. The peak of the energy generation occurs at a temperature of about 14×10^6 K and a density of about $95\,\mathrm{gcm^{-3}}$.

†Appendix A of Bahcall *et al.* (1982) defines S and discusses the initial steps in the construction of the model. S determines the adiabat of the convection zone. In earlier treatments of the problem, one adjusted the constant $K = P/T^{2.5}$, which gives the relation between pressure and temperature in the convective envelope [see Sears (1964) or Bahcall and Shaviv (1968)].

‡The precise parameters for the convective zone are unimportant for the solar neutrino problem although they are important for the calculation of the p-mode oscillation frequencies.

https://doi.org/10.1017/S0252921100067798 Published online by Cambridge University Press

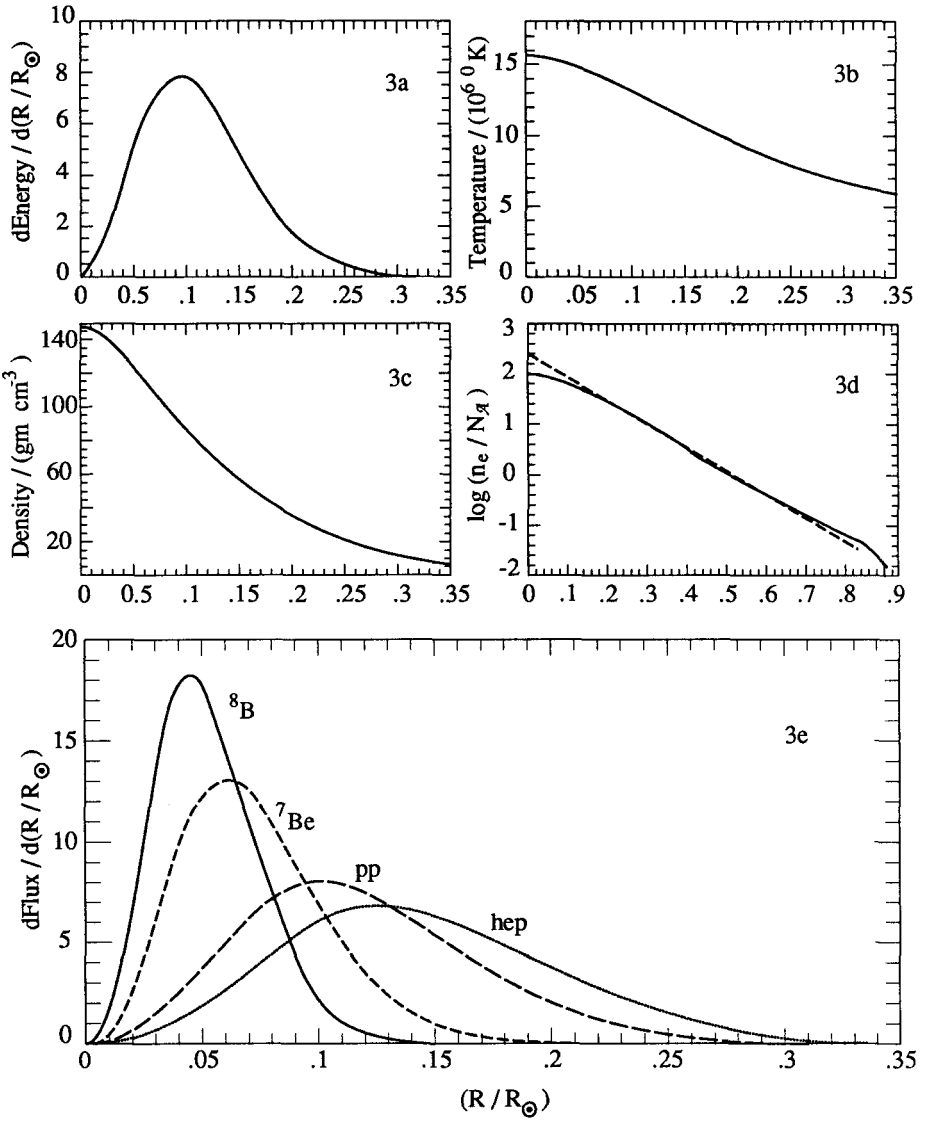

Figure 3. Radial profiles of physical parameters in the standard solar model. Fig 3*a* shows the fraction of the energy generation that is produced at each position. Fig 3*b* illustrates the temperature distribution. Fig 3*c* illustrates the density distribution. Fig 3*d* shows as a solid line the logarithm of the electron number density, N_e, divided by Avogadro's number, $N_{\mathcal{A}}$, as a function of solar radius. The dotted line is an exponential fit to the density distribution. Fig 3*e* represents the neutrino production as a function of radius for ^{8}B, ^{7}Be, pp and hep neutrinos. [Reproduced with permission of the publisher from *Neutrino Astrophysics* by J. N. Bahcall, Cambridge University Press (1989).

https://doi.org/10.1017/S0252921100067798 Published online by Cambridge University Press

The dependence of the electron number density upon solar radius is shown in Figure 3*d*; these density is an important input for the MSW effect [Smirnov (1989)]. The equation of the dotted line (fit of a linear function) is :

$$n_e/N_A = 245 \exp(-10.54x) \text{ cm}^{-3}, \quad (7)$$

where $x = R/R_\odot$. Note that the linear fit is not exact and the parameters depend upon where the fitting is done. In particular, the formula given in Eq. (7) gives a value of n_e that is too large by about a factor of 2.5 at the solar center.

Figure 3*e* shows where in the sun the different neutrinos originate. The comparison with the others figures shows clearly that the pp flux is produced in the same region than the energy. Because of its strong temperature dependence, the ^{8}B production is peaked at much smaller radii, $.05R_\odot$. ^{7}Be is intermediate between pp and ^{8}B. The hep production is the most extended, and reflect the ^{3}He abundance increase as one goes outward from the center.

Helium is increased in abundance with respect to hydrogen by nuclear burning in the solar interior. In the innermost region, the ^{3}He abundance is small because ^{3}He is burned rapidly by reactions 3 and 4 of Table 2. In the outermost region, no ^{3}He is produced by proton burning. Thus, there is a sharp peak in the ^{3}He abundance near $0.28R_\odot$. The helium mass fraction is highest in the interior as the result of hydrogen burning, while the heavy element abundance is constant everywhere, by assumption. In all of the modern calculations, the core of the Sun is convectively stable, although not by much.

The model of the present Sun has a luminosity that has increased by 41% from the nominal zero-age model (when the model Sun first reached quasistatic equilibrium on the main sequence) and the effective temperature has increased by 3%. The flux of ^{8}B neutrinos has increased dramatically; the contemporary flux is a factor of 41 times larger than the zero-age value.

The largest recognized contribution to the uncertainty in the inferred helium abundance is caused by the uncertainty in the initial value of Z/X and is of order a few percent. Standard solar models yield a well-defined value for the initial helium abundance:

$$Y = 0.27 \pm 0.01. \quad (8)$$

This initial solar value of helium represents an upper limit to the primordial helium abundance at the beginning of the Big Bang. Three determinations of the helium abundance are in satisfactory agreement: the initial solar helium abundance, the present-day abundance of helium in the Galaxy's interstellar medium, and the preferred abundance based on cosmological considerations. All three quantities are equal to within the errors of their determinations, which are at least a few percent.

5. Solar neutrinos

Is there really a solar neutrino problem? The answer is yes if the difference between the predicted and the measured capture rates exceeds the range of the uncertainties. The answer is no if the uncertainties exceed the discrepancy between theory and observation.

The solar neutrino fluxes as well as the uncertainties, calculated from the standard solar model are shown in first row of Table 4.

The flux of the basic pp neutrinos can be calculated to an estimated accuracy of 2% using the standard solar model. Thus the pp flux, the dominant flux of solar neutrinos,

https://doi.org/10.1017/S0252921100067798 Published online by Cambridge University Press

Table 4. Calculated solar neutrino fluxes and predicted capture rates for ^{37}Cl and ^{71}Ga detectors .

Source	Flux (10^{10} cm^{-2} s^{-1})	Capture rate ^{37}Cl	Capture rate ^{71}Ga
pp	6.0 (1 ± 0.02)	0.0	70.8
pep	0.014 (1 ± 0.05)	0.2	3.0
hep	8×10^{-7}	0.03	0.06
^{7}Be	0.47 (1 ± 0.15)	1.1	34.3
^{8}B	5.8×10^{-4} (1 ± 0.37)	6.1	14.0
^{13}N	0.06 (1 ± 0.50)	0.1	3.8
^{15}O	0.05 (1 ± 0.58)	0.3	6.1
^{17}F	5.2×10^{-4} (1 ± 0.46)	0.003	0.06
Total		7.9 SNU	132^{+20}_{-17} SNU

can be thought of as a reliable source, placed at an astronomical distance, which can be used for physical experiments on the propagation of neutrinos.

The production rate for the rare neutrinos from ^{8}B β-decay is sensitive to conditions in the solar interior, because of the relatively high Coulomb barrier for the ^{7}Be(p,γ)^{8}B reaction ($\sim$ 10 MeV compared to a mean thermal energy of 1 keV). The calculated flux of ^{7}Be electron capture neutrinos is intermediate in sensitivity between the pp and the ^{8}B neutrinos.

The calculated uncertainties are described in terms of a total theoretical range. The calculation of a *true* "three standard deviation level of confidence," cannot be done because the probability distribution is unknown for parameters that must be calculated, not measured (e.g., radiative opacity or higher-order corrections to neutrino cross sections). In practice, the meaning of the total theoretical range is that, if the true value lies outside this range, someone who has determined an input parameter (experimentally or theoretically) has made a mistake.

For measured quantities (e.g., nuclear reaction rates), we use standard 3σ limits to estimate the uncertainties. For theoretical quantities, we usually take the uncertainties in quantities that are calculated to be equal to the range in values in published state-of-the-art calculations, especially when this range exceeds (as it usually does) the published estimates of uncertainties. (Of course, the theory could be wrong in some fundamental way that would not be reflected in scatter in the values obtained by different treatments.) Quantities for which only one calculation is available require a more delicate judgment. For example, we have chosen to multiply the value of higher-order corrections to neutrino capture cross sections by three and call this the total uncertainty. It is possible that we assign relatively larger errors for experimentally determined parameters (for which the errors are more easily quantifiable) than we do for the calculated parameters such as the opacity. However, the adopted procedure is as objective as any we can think of and has the advantage of simplicity.

Figure 4 shows the predicted capture rates for the ^{37}Cl experiment as a function of the date of publication for each paper published by the author (1963 to 1988). The original

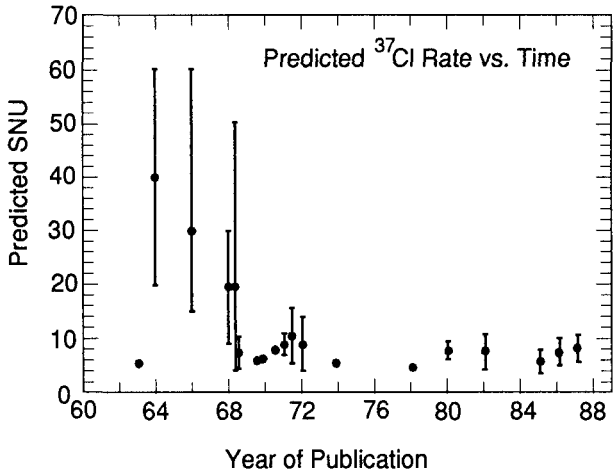

Figure 4. Predicted capture rates as a function of time. The published predictions of the author and his collaborators of neutrino capture rates in the ^{37}Cl experiment are shown as a function of the date of publication. [Reproduced with permission of the publisher from *Neutrino Astrophysics* by J. N. Bahcall, Cambridge University Press (1989).]

error bars are shown for every case in which they were published. All 14 values published since 1968 are consistent with the range given in Eq. (1.a).

The discussion up to this point has emphasized the theory of neutrino emission from the Sun. Fortunately, this theory can be tested observationally.

5.1 The ^{37}Cl experiment

The beautiful ^{37}Cl experiment of Davis and his collaborators was for two decades the only operating solar neutrino detector. The reaction that is used for the detection of the neutrinos is:

$$\nu_e + {}^{37}\mathrm{Cl} \Rightarrow e^- + {}^{37}\mathrm{Ar}, \tag{9}$$

which has a threshold energy of 0.8 MeV. The target is a tank containing 615 tons of C_2Cl_4), deep in the Homestake Gold Mine in Lead, South Dakota. The average rate at which ^{37}Ar is produced is

$$\text{Production rate} = 0.543 \pm 0.035 \text{ atoms day}^{-1}, \tag{10a}$$

of which a small part is background (from cosmic ray events),

$$\text{Background rate} = 0.08 \pm 0.03 \text{ atoms day}^{-1}. \tag{10b}$$

Subtracting the known background rate from the production rate yields the capture rate

$$\text{Capture rate} = (2.33 \pm 0.25) \text{ SNU}, \tag{10c}$$

which is due to solar neutrinos if all of the significant contributions to the background have been recognized. The errors quoted in these three observed rates are all 1σ uncertainties.

The ^{37}Cl experiment is discussed in more detail in this book [Davis (1989)].

https://doi.org/10.1017/S0252921100067798 Published online by Cambridge University Press

5.2 *The Kamiokande II experiment*

The Kamiokande II experiment, which is located in the Japanese Alps, detects Cerenkov light emitted by electrons that are scattered in the forward direction by solar neutrinos. The reaction by which the neutrinos are observed is

$$\nu + e \rightarrow \nu' + e', \tag{11}$$

where the primes on the outgoing particle symbols indicate that the momentum and energy of each particle can be changed by the scattering interactions. For the higher-energy neutrinos (> 5 MeV, i.e., ^{8}B and hep neutrinos only) that can be observed by this process using available techniques, the scattering provides additional information not available with a radiochemical detector. Neutrino–electron scattering experiments furnish information about the incident neutrino energy spectrum (from measurements of the recoil energies of the scattered electrons), determine the direction from which the neutrinos arrive, and record the precise time of each event.

The preliminary results discussed at this Conference [Nakahata (1989), Hirata et al. (1989)], from the Kamiokande II detector, yield a ^{8}B neutrino flux that is approximately 0.39 of the standard model flux, about 3σ away from zero and from the standard model value. This result applies for recoil electrons with a minimum total energy of 7.5 MeV. A significant forward peaking of the recoil electrons is observed along the direction of the Earth–Sun axis. This result is of great importance since all of the previous observational results on solar neutrinos came from a single ^{37}Cl experiment.

5.3 *Gallium detectors*

Two radiochemical solar neutrino experiments using ^{71}Ga as a target are under way. The GALLEX collaboration uses 30 tons of gallium in an aqueous solution; the detector is located in the Gran Sasso Underground Laboratory in Italy [Kirsten (1989)]. The Soviet-American experiment, SAGE, uses about 60 tons of gallium metal; the solar neutrino laboratory is constructed underneath a high mountain in the Baksan Valley in the Caucasus Mountains of the Soviet Union [Gavrin (1989)].

The gallium experiments can furnish unique and fundamental information about nuclear processes in the solar interior and about neutrino propagation. The neutrino absorption reaction is:

$$\nu_e + {}^{71}\mathrm{Ga} \Rightarrow e^- + {}^{71}\mathrm{Ge}. \tag{12}$$

The germanium atoms are removed from the gallium and the radioactive decays of ^{71}Ge (half-life 11.4 days) are measured in small proportional counters. The threshold for absorption of neutrinos by ^{71}Ga is 0.233 MeV, which is well below the maximum energy of the pp neutrinos.

Table 4 shows the calculated contribution from individual neutrino sources to the predicted capture rate. Neutrinos from the basic pp reaction are expected, according to the standard model, to produce approximately half of the computed total capture rate. The other main contributors are ^{7}Be neutrinos, about one-quarter of the total rate, and ^{8}B neutrinos, about 10%.

6. Helioseismology

Helioseismology, like terrestrial seismology, provides information about the interior of the body under study by using observations of slight motions on the surface. The technique is analogous to striking a bell and using the frequencies of the emitted sound to make inferences about the bell's constitution. Leighton, Noyes, and Simon (1962) first discovered solar oscillations by studying the velocity shifts in absorption lines formed in the solar surface. They found that the surface of the Sun is filled with patches that oscillate intermittently with periods of the order of 5 minutes and velocity amplitudes of order 0.5 $\mathrm{km\,s^{-1}}$. The oscillatory motion was subsequently detected in measurements of the solar intensity. The oscillations typically persist for several periods with a spatial coherence of order a few percent of the solar diameter.

We now know [Ulrich (1970) and Leibacher and Stein (1971)] that the Sun acts as a resonant cavity. Sound waves known as **p-modes** (or pressure modes, because the restoring forces is the compressibility of gases) are largely trapped between the solar surface and the lower boundary of the convection zone. The waves bounce back and forth between spherical-shell resonant cavities bounded on the outside by the reflections due to the density gradient near the solar surface and on the inside by refractions due to the increasing sound speed.

In order for a mode to resonate in the solar acoustic cavity, a half-integral number of waves must fit along the path leading from the solar surface to the base of the cavity. The depth of the cavity is fixed by the condition that horizontal wavenumber equals the total wavenumber (i.e., the vertical wavenumber becomes equal to zero), at which point the wave is refracted back towards the surface. The vertical wavenumber decreases with increasing depth in the Sun because the temperature rises in the inner regions. For many of the waves that have been most intensively studied, the base of the resonant cavity is close to the base of the convective zone.

For a given horizontal wavelength only certain periods will correspond to a resonance in the solar cavity. It was therefore predicted [Ulrich (1970)] and subsequently observed [Deubner (1975) and Rhodes, Ulrich, and Simon (1977)] that the strongest solar oscillations fall in a series of narrow bands when the results are displayed in a two-dimensional power spectrum that shows amplitude as a function of both period and horizontal wavelength. Just as in a musical instrument, the largest amplitudes correspond to standing waves that constructively interfere at the boundaries of the cavity. Solar rotation breaks the symmetry between otherwise degenerate modes and enables observers and theorists working together to make important inferences about the rate at which interior regions of the Sun are rotating.

Observations by Claverie *et al.* (1979) and by Grec, Fossat, and Pomerantz (1980), which utilized the integrated light from the entire solar disk, showed that the oscillations are globally coherent. The modes observed by these techniques provide the most important information currently available for the study of the deep solar interior since they penetrate most deeply toward the solar center.

The stability of the oscillations sets a limit on the precision of the helioseismological constraints that we can impose on the solar models. Present observations indicate that the frequencies of the oscillations can be measured to an accuracy of about two parts in ten thousand, which provides strong constraints. Indeed, some of the earliest detailed observational results led to the conclusion that the depth of the solar convec-

tion zone was somewhat greater than previously believed [Gough (1977) and Rhodes, Ulrich, and Simon (1977)].

The p-mode frequencies are insensitive to even a drastic change in nuclear energy generation. For example, the characteristic change in p-mode frequencies caused by switching off the ^{3}He + ^{4}He reaction (and all the higher-energy neutrino fluxes) is less than 0.01% [see Bahcall and Ulrich (1988)].

The frequencies of the **g-mode** [or gravity waves, with gravity as restoring force], which penetrate deeply into the stellar interior, exhibit a small sensitivity ($\sim 0.2\%$) to the hypothetical change in nuclear energy generation. There have been several reports suggesting that g-modes may have been detected in the Sun, but these claims are controversial.

The calculations using the standard solar model represent well the quantitative features of the solar p-mode frequency spectrum. However, there are small ($\sim$ a few tenths of a percent) discrepancies between observations and calculations of typical p-mode splittings, which are of order 10^2 μHz. The most significant discrepancy is the difference between the calculated and observed value of δ_{02} , the small (~ 10 μHz) frequency separation (for radial nodes n differing by 1) between the modes with spherical harmonic degrees $l = 0$ and $l = 2$. There are theoretical reasons for believing that this frequency separation, related to the gradient of the sound speed in the interior of the sun, is less susceptible to uncertain surface phenomena than are the much larger frequency splittings. Bahcall and Ulrich (1988) estimate the discrepancy to be at approximately the 3σ level of significance. The observed value for δ_{02} is between 8.9 μHz and 9.9 μHz [Pallé *et al.* (1987)], depending upon the pairs of radial nodes chosen. The value calculated with the standard solar model is 10.6 μHz.

A small gradient in the initial helium abundance can modify the calculated oscillation frequencies significantly and in the correct sense to improve the agreement with observations [see rows 14 through 17 of Table XX of Bahcall and Ulrich (1988)]. The calculated ^{8}B neutrino flux is thus only increased by about 15% by this specified *ad hoc* assumption regarding the composition gradient, an amount that is smaller than the currently estimated uncertainties in calculating the neutrino fluxes.

The histogram of the fractional contributions to the observed p-mode splitting is shown in Figure 5 for mass fractions from $0.05M_\odot$ to $1.0M_\odot$, corresponding to radial intervals from $0.08R_\odot$ to $1.0R_\odot$. The histograms for the production of neutrinos from ^{8}B decay and the generation of the solar luminosity (which is nearly the same as the histogram for the production of neutrinos from the pp reaction) are also displayed in Figure 5.

Figure 5 shows that the three observational quantities, p-mode oscillations, the solar luminosity (or pp neutrinos), and ^{8}B neutrinos, are primarily determined in different regions. Nearly all of the neutrinos from ^{8}B decay originate in the inner 5% of the solar mass. Almost 70% of the p-mode splitting comes from the outer 10% of the solar mass. The important regions for the generation of the solar luminosity, and the flux of neutrinos from the pp reaction, are intermediate in distribution between those for the p-mode splitting and those for the flux of ^{8}B neutrinos.

7. Conclusion

The studies of solar neutrinos and of p-mode oscillations are largely complementary. Both techniques are required in order to understand the solar interior and both kinds of studies have influenced work in the complementary field.

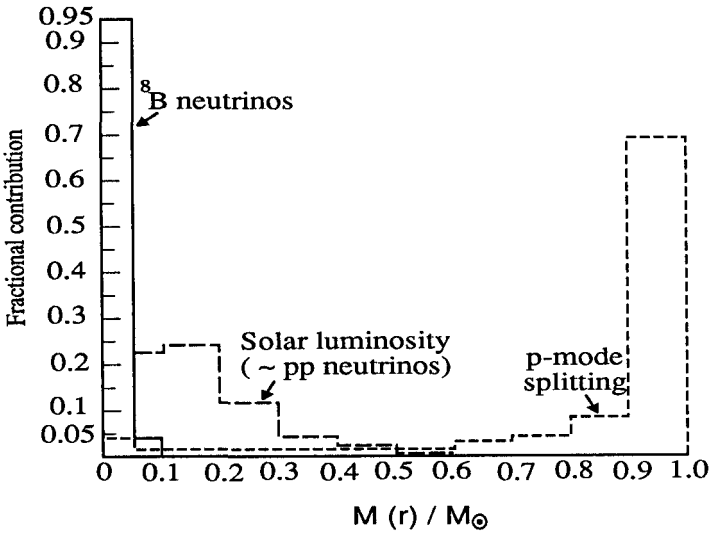

Figure 5. Histogram of fractional contributions to p-mode splitting, the flux of neutrinos from ^{8}B decay, and the flux of neutrinos from the pp reaction. Here $M(r)/M$ is the fraction of the solar mass interior to the point r. In order to resolve the ^{8}B neutrino emission, the width of the inner two histogram points is $0.05M(r)/M$, not $0.1M(r)/M$. [Reproduced with permission of the publisher from *Neutrino Astrophysics* by J. N. Bahcall, Cambridge University Press (1989).]

Solar models that involve WIMPs [see Spergel (1989)] may, according to some authors, improve agreement with p-mode oscillation measurements and reduce by a large factor the predicted ^{8}B neutrino fluxes. In the same time they could account for the dark matter needed to fill the universe.

A review of non-standard solar models, proposed in the context of the solar neutrino problems is given by Maeder (1989); the precision of most of the calculations in the literature, which is much less than for the standard solar model, makes difficult the comparison with observational results. Nevertheless comparison with the tight experimental constraints that are now being obtained in the study of helioseismology can greatly reduce the number of these "non-standard" solar models.

In the near future new data will be available. Solar neutrinos experiments will be sensitive to pp-neutrinos - Gallex or Sage - or able to measure in real time the energy spectrum [Spiro (1989)]. In helioseismology, with the advent of large networks of solar observatories around the earth [Hill (1989)] or in space [Bonnet (1989)], new constraints will be put on opacities [Cox (1989)].

If the solution of the solar neutrino problem is not in the field of astrophysics it could be in the properties of neutrinos. Indeed the problem takes another dimension with the MSW effect which is able to modify the energy spectrum of the neutrino emitted by the Sun [Smirnov (1989)]. This allows to test very small masses of neutrinos which are in the range of the predictions made by Grand Unified Theories [Harari (1989)].

Will solar neutrinos be the low-energy frontier of high-energy physics ? If MSW is the correct explanation, then information about the grand unification mass scale at 10^{15} GeV could be obtained from interaction of neutrinos driven by mass differences of 10^{-20} GeV !

References

Aller, L., H. (1986), in *Spectroscopy of Astrophysical Plasmas,* edited by A. Dalgarno and D. Layzer (Cambridge University Press, Cambridge, England), p.89.

Bahcall, J. N. (1989), *Neutrino Astrophysics*, (Cambridge University Press, Cambridge, England).

Bahcall, J.N. and G.Shaviv (1968) *Ap. J.*, **153**, 113

Bahcall, J.N., N.A. Bahcall, and R.K. Ulrich (1969) *Ap. J.*, **156**, 559.

Bahcall, J.N. (1978) *Rev. Mod. Phys.*, **50**, 881.

Bahcall, J.N., W.F. Huebner, S.H. Lubow, P.D. Parker, and R.K. Ulrich (1982) *Rev. Mod. Phys.*, **54**, 767.

Bahcall, J.N. and R.K. Ulrich (1988) *Rev. Mod. Phys.*, **60**, 297.

Bonnet, R.M. (1989) *These proceedings.*

Claverie, A., G.R. Isaak, C.P. McLeod, H.B. van der Raay, and T. Roca Cortes, (1979) *Nature,* **282**, 591

Cox, A.N., J.A. Gusik and R.B. Kidman (1989) *Ap. J.*, **999**, 999

R. Davis (1989) *These proceedings.*

Deubner, F.-L. (1975) *Solar Phys.*, **44**, 371.

Dicke, R.H., J.R. Kuhn and K.G. Libbrecht (1985) *Nature*, **316**, 687

Gavrin, V.N. (1989) *These proceedings.*

Gough, D.O. (1977), in *The Energy Balance and Hydrodynamics of the Solar Chromosphere and Corona,*edited by R.M. Bonnet and P. Delache (de Bussex, Clermont-Ferrand), p.3.

Grec, G., E. Fossat and M.A. Pomerantz (1980) *Nature*, **288**, 541

Grevesse, N. (1984) *Physica Scripta*, **T8**, 49.

Harari, H. (1989) *These proceedings.*

Hayashi, C. (1961) *Pub. Astro. Soc. Japan*, **13**, 450

Hayashi, C. (1966) *Ann. Rev. Astron. Astrophys.*, **4**, 171

Hirata, K. S., et al. (1989) KEK preprint 89-63.

Huebner, W.F. (1986) in *Physics of the Sun,* edited by P.A. Sturrock, T.E. Holzer, D.M. Mihala, and R.K. Ulrich (Dordrecht: Reidel)

Iglesias, C.A. (1989) *These proceedings.*

Kirsten, T. (1989) *These proceedings.*

Leibacher, J.W. and R.F. Stein (1971) *Astrophys. Lett.*, **7**, 191.

Leighton, R.B., R.W. Noyes, and G.W. Simon (1962) *Ap. J.*, **135**, 474.

Maeder, A. (1989) *These proceedings.*

Nakahata, M. (1989) *These proceedings.*

Pallé, P., J.C. Perez, C. Regulo, T. Roca Cortes, G.R. Isaak, C.P. McLeod, and H.B. van der Raay (1979) *Astron. Astrophys.*, **170**, 114

Parker, P. D. and Rolfs, C. (1989) *These proceedings.*

Rakavy, G., G. Shaviv and A. Zinamon (1967) *Ap. J.*, **150**, 131
Rhodes, E.J., Jr., R.K. Ulrich and G.W. Simon (1977) *Ap. J.*, **218**, 901
Sears, R.L. (1964) *Ap. J.*, **140**, 477.
Schwarzschild, M. (1958) *Structure and Evolution of the Stars* (Princeton University Press)
Sienkiewicz, R., Bahcall, J. N., and Paczynski, B. (1989), *Ap. J.* (December).
Smirnov, A. (1989) *These proceedings.*
Spergel, D.N. (1989) *These proceedings.*
Spiro, M. and D. Vignaud (1989) *These proceedings.*
Turck-Chièze, S., S. Cahen, M. Cassé and C. Doom (1988) *Ap. J.*, **335**, 415
Ulrich, R.K. (1970) *Ap. J.*, **162**, 993.
Ulrich, R.K. (1982) *Ap. J.*, **258**, 404.